Energy balance closure at global eddy covariance research sites is related to landscape-level surface heterogeneity

Paul C. Stoy[1], **others**

[1] Department of Land Resources and Environmental Science, Montana State University, Bozeman, MT, USA

Corresponding Author:	Paul Stoy
Address:	Department of Land Resources and Environmental Science, Montana State University, Bozeman, MT
Phone:	406 600 3577
Email:	paul.stoy@montana.edu

Journal:	Agricultural and Forest Meteorology
Running title:	Global surface radiation and water flux
Keywords:	Eddy covariance, Enhanced vegetation index, FLUXNET, MODIS, Plant functional type, Radiation balance closure

Abstract

The lack of radiation balance closure in many eddy covariance research sites is a major impediment to surface-atmosphere water and radiation flux research. A recent synthesis by Foken (2008, *Ecological Applications*, 18(6): 1351–1367) identified exchange processes and turbulent motions at large spatial and temporal scales in heterogeneous landscapes as the primary cause of lack of energy balance closure at select, intensively-researched sites. We investigated the relationship between landscape heterogeneity and radiation balance closure at 180 eddy covariance research sites in the FLUXNET database using remote sensing products from MODIS. Plant functional type variability, as quantified by its entropy, in the 20 × 20 km area surrounding flux towers was significantly related to energy balance closure ($p = 0.011$) as was the landscape-level variability of enhanced vegetation index quantified by its variance ($p = 0.038$). Energy balance closure averaged 0.83 across all sites investigated here, but 0.89 for sites with near-uniform plant functional type variability at the landscape scale. These results agree with previous studies and suggest that the role of landscape-level heterogeneity in influencing mesoscale meteorological motions in heterogeneous landscapes must be investigated, in addition to all heat storage terms, to close the radiation balance at surface flux observation towers.

Introduction

The surface-atmosphere exchanges of radiation, momentum, water and trace gases are central components of the Earth system. Nearly one thousand years of eddy covariance and micrometeorological observations from diverse global ecosystems have been organized from regional measurement networks [e.g. (Aubinet et al., 2000; Li et al., 2005)] to create the FLUXNET database (Baldocchi et al., 2001; Papale et al., 2006). Most FLUXNET studies seek to understand the biosphere-atmosphere flux of CO_2 in relation to climate, radiation and hydrology across time in single ecosystems, across ecosystem types, or in global ecosystems [e.g. (Baldocchi, 2008; Law et al., 2002)]. Fewer studies to date have investigated global and regional water and energy fluxes, apart from their relationship to CO_2 flux [but see, for example Falge *et al.* (2001), Hollinger *et al.* (2009), Law *et al.* (2002)], despite their importance to hydrology and the climate system.

A major reason for the relative lack of water and energy balance studies that rely on eddy covariance data is concerns over the lack of radiation balance closure at most research sites (Aubinet et al., 2000; Wilson et al., 2002). Multi-site syntheses do date found an average of radiation balance closure about 0.80-0.85 (Li et al., 2005; Wilson et al., 2002), with individual or multiple sites reporting better (Barr et al., 2006) or worse closure (Stoy et al., 2006) or, in rare cases, near-to-full closure (Heusinkveld et al., 2004; Lindroth et al., 2009; Vourlitis and Oechel, 1999). Considering other contributions to ecosystem heat storage reduces the closure problem (Heusinkveld et al., 2004; Lindroth et al., 2009; Meyers and Hollinger, 2004), but additional measurements often prove ineffective for closing the radiation balance (Aubinet et al., 2010) and large field campaigns rarely report full closure [see Table 2 in Foken (2008)]. Foken (2008) provided a historical overview and modern synthesis of the energy balance closure problem and concluded that turbulent structures resulting from the landscape heterogeneity are likely responsible for energy imbalance at the tower measurement level following remote sensing investigations by Mauder *et al.* (2007). Here, we test the hypothesis that energy balance closure is related to landscape heterogeneity, using data from 180 global eddy covariance research sites using products from the MODIS platform surrounding flux tower locations after discussing the energy balance closure characteristics of the FLUXNET database.

Methods

FLUXNET

Flux and meteorological data from version 2 of the LaThuile FLUXNET database [www.fluxdata.org, accessed May 31, 2008], and processed according to FLUXNET protocol, (Papale et al., 2006; Reichstein et al., 2005), was used. For the analysis of landscape heterogeneity on energy balance closure, we explore the 180 (of 253) sites with observations of net radiation (R_n), latent heat flux (λE), sensible heat flux (H) and soil heat flux (G)

(Table 1, Figure 1) for which the sum of available energy ($\sum(R_n - G)$) is positive over the observation period. For the purposes of this analysis, we define the closure of the radiation balance (C_{EB}) as:

$$C_{EB} = \frac{\sum(\lambda E + H)}{\sum(R_n - G)} \tag{2}$$

i.e. the fraction of available energy ($\sum(R_n - G)$) that is observed as a surface flux ($\sum(\lambda E + H)$). C_{EB} also commonly called the energy balance ratio (Wilson et al., 2002). Half-hourly data for which the quality control flags for R_n, λE, H, and G are all equal to 1 (indicating measured, quality-controlled data that are not gapfilled) were converted from W m^{-2} to MJ m^{-2} half hour^{-1} and summed for the calculation of C_{EB}. Heat storage in the canopy air space and aboveground vegetation and any metabolic terms are assumed to be minor for the purposes of this study, not because we believe that these terms are not important (Gu et al., 2007; Lindroth et al., 2009), but rather because information on sensor height and canopy volume is not readily available in the FLUXNET ancillary database. C_{EB} is therefore the best estimate given the available data, but can be expected to be somewhat less than unity in this study. For the statistical analyses, we treat each FLUXNET site, not site-year, as independent.

MODIS: Land Cover Classifications

Following the suggestions of Foken (2008), the landscape characteristics of the 20 $\times$ 20 km area surrounding the 180 flux towers were analyzed in relation to C_{EB}. The MODIS MCD12Q1 land cover classification products are annual products and we investigate the IGBP (International Geosphere-Biosphere Program), UMD (University of Maryland), LAIfPAR (Leaf Area Index/Fraction of Absorbed PAR), and PFT (Plant Functional Type) for landscapes surrounding tower locations for 2006. As these data are categorical, an appropriate metric for their variability is their information entropy after Shannon (1948):

$$\mathrm{H(X)} = -\sum_{i=1}^{N} p(x_i)\log p(x_i) \tag{3}$$

where N is the number of bins that a pixel can take for each attribute. For example, there are 12 classifications for PFT (water = 0, evergreen needleleaf trees = 1, evergreen broadleaf trees = 2, etc.), therefore N = 12 and the Shannon entropy of a uniform landscape of a single plant functional type would be:

$$\mathrm{H}(\mathrm{X}) = -\sum_{i=1}^{12} p(x_i) \log p(x_i) = -(12-1) \times 0 - 1 \times \log(1) = 0. \quad (4)$$

Unfilled and unknown MODIS pixels were ignored in the entropy calculations.

MODIS: Enhanced Vegetation Index

We chose the MODIS product with the highest spatial resolution, 250 m in the MOD13Q1 product, for the calculation of EVI in the 20 $\times$ 20 km area surrounding the 180 study flux towers. The 16 day resolution of the MOD13Q1 EVI product creates a challenge for quantifying a simple metric of landscape-level variability; we obtained EVI images for each site for three year period 2005-2007 and chose the scene with the largest amount of reliable data that had the highest mean EVI in order to calculate landscape-level variability during the growing season period when incident radiation is on average highest. The variance of the selected scene, $\sigma^2(EVI)$, is used as the metric of landscape-level heterogeneity in subsequent analyses.

Results

Energy balance closure

The average C_{EB} for the 180 sites listed in Table 1 is 0.83 with a relatively large variability (standard deviation) of 0.25 (Figure 1, Figure 2A). From the probability density functions in Figure 2A, a number of sites with extremely low (0.5) and high (1.2, especially the extreme cases over 2) may be excluded for data quality concerns, leaving 161 sites with C_{EB} = 0.83 ± 0.14 for the subsequent statistical analyses.

Table 2 lists energy balance closure for different ecosystem types. Ignoring outliers (noting values in parentheses), evergreen broadleaf forests, grasslands, savannas and shrubs have the highest values of C_{EB} and deciduous broadleaf forests, mixed forests, and wetlands the lowest.

Forests tend to have lower average energy balance closure (C_{EB} = 0.80) than shorter-statured vegetation (crops, grasslands and shrubs; C_{EB} = 0.85, Figure 2B), but this difference is not significant for the sites chosen here (two-sided t-test, p=0.065).

Landscape heterogeneity

MODIS PFT and EVI for the 20 $\times$ 20 km area surrounding the tower in Hainich Forest, Germany are shown in Figures 3 and 4, respectively, as examples. For reference, H(PFT) for Figure 3 is 0.90 and $\sigma^2(EVI)$ for Figure 4 is 8.6×10^{-3}

The relationship between C_{EB} and H(IGBP), H(UMD), H(LAIfPAR) and H(PFT) trends negative, indicating lower energy balance closure in more variable landscapes, but, after performing the Bonferroni adjustment for multiple (4) hypothesis tests, p=0.05/4=0.012, and only the relationship between H(PFT) and C_{EB} is significant at the 5% level (p=0.011); the p-values between C_{EB} and H(IGBP), H(UMD) and H(LAIfPAR) are 0.054, 0.11, and 0.043, respectively. Interestingly, the intercept for each landscape classification entropy and C_{EB} is between 0.87 and 0.89, suggesting that radiation balance closure approaches *ca.* 0.9 in uniform landscapes. $\sigma^2(EVI)$ has a significant negative relationship with C_{EB} (r=-0.16; p=0.040) even after excluding obvious outliers [$\sigma^2(EVI)$>0.04] that may have spuriously influenced this relationship (r=-0.16; p=0.043).

Discussion

Energy balance closure

Energy balance closure of the 180 FLUXNET sites investigated here (0.83) is on the order of previous multi-site synthesis [0.79, ranging from 0.53 to 0.99, (Wilson et al., 2002); 0.84, ranging from 0.58 to 1 (Li et al., 2005; Yu et al., 2006)] if not slightly worse than syntheses from multiple sites of a single ecosystem type [0.85-0.89, (Barr et al., 2006)]. Forests tend to have lower closure than short-statured vegetation, due in part to the role of heat storage in the canopy and canopy air space. Incorporating these terms and the storage of heat above the soil heat flux sensors can be expected to improve closure (Cava et al., 2008; Meyers and

Hollinger, 2004) but would require modelling for the present analysis, which seeks to synthesize available radiation balance closure measurements.

Landscape heterogeneity

Foken (2008) discussed the results of multiple large surface flux campaigns and argued that the problem of eddy covariance radiation balance closure is fundamentally a problem of scale: lower frequency motions (Foken et al., 2006), possibly resulting from surface heterogeneity at the landscape scale (Foken, 2008), explain in part the lack of radiation balance closure. The results here agree with his conclusions; C_{BE} in globally-distributed flux towers (Table 1) is significantly related to the variability of PFT and EVI on the scale of landscapes surrounding flux towers (Figure 5), despite differences in flux measurements, tower design, and sensor placement, in globally-distributed flux towers.

The best strategy for including the flux information contained in larger atmospheric motions remains to be discovered. Longer averaging periods are frequently cited (Cava et al., 2008; Malhi et al., 1998), but this comes at the expense of capturing the diurnal variability in flux. Turbulent organized structures (Kanda et al., 2004; Steinfeld et al., 2006) may simplify energy balance closure if simple parameterizations can be found. The influence of differential atmospheric heating due to differences in vegetation characteristics needs to be further investigated to quantify the role of surface heterogeneity in boundary-layer turbulence.

It has been noted previously that C_{EB} is greater in unstable atmospheres (Stoy et al., 2006) [sometimes quantified by the Richardson number, (Lindroth et al., 2009)] in addition to the more commonly-reported relationship with the friction velocity [u*, e.g. Barr *et al.* (2006)]. A plausible explanation for the lack of radiation balance closure in these instances is boundary layer entrainment, which would transfer air parcels from the free atmosphere that are likely colder but only occasionally wetter than the planetary boundary layer. It may be argued that such events bias surface-atmosphere H measurements more than λE [see Appendix C in Stoy *et al.* (2006)]. This hypothesis merely represents a conjecture that requires future work, but we note that efforts to close the surface water balance using multiple measurement strategies including eddy covariance usually agree (Oishi et al., 2008; Schäfer et al., 2002), suggesting that bias in eddy covariance-measured λE is low. Other studies suggest partitioning the residual energy equally to H and λE following the Bowen ratio (Lee, 1998; Twine et al., 2000) as a null assumption for the 'missing' energy, but such a correction relies on similarity assumptions that are not supported by low frequency spectra (Ruppert et al., 2006), suggesting that fluxes should not be corrected based on the energy balance residual until the issue of low frequency eddies are resolved (Baldocchi, 2008). Work on larger atmospheric motions must continue to progress in our understanding of the surface radiation balance (Foken, 2008)

Conclusions

We acknowledge that combining additional heat flux and storage measurements and models to existing tower sites will reduce, but not remove, the problem of energy balance closure given that no large surface flux campaign has reported full energy balance closure to date [see Table 2 in Foken (2008)]. The leading hypothesis from comprehensive surface flux investigations is that larger atmospheric motions, potentially driven by surface heterogeneity, are the principal explanation for lack of closure. The present study agrees with this hypothesis to the extent that a data-driven study can investigate the problem; C_{BE} in globally-distributed flux towers is significantly related landscape-level heterogeneity in surface type (via PFT) and characteristics (via EVI). Other metrics investigated (IGBP, UMD, NEEfPAR) demonstrate trends with C_{BE} that may relate more strongly with C_{BE} if additional factors like topography are included. The physical explanations behind the relationship between energy balance closure and landscape heterogeneity should be investigated further to add value to the water and energy flux observations in the FLUXNET database and to finally bring closure to the energy balance closure problem.

Acknowledgements

We would first and foremost like to acknowledge the FLUXNET data providers and the organizers of the FLUXNET database. This work is an outcome of the La Thuile FLUXNET workshop 2007, which would not have been possible without the financial support provided by CarboEuropeIP, FAOGTOS-

TCO, iLEAPS, Max Planck Institute for Biogeochemistry, National Science Foundation, University of Tuscia, and the U.S. Department of Energy. The Berkeley Water Center, Lawrence Berkeley National Laboratory, Microsoft Research eScience, Oak Ridge National Laboratory provided databasing and technical support. The AmeriFlux, AfriFlux, AsiaFlux, CarboAfrica, CarboEuropeIP, ChinaFlux, Fluxnet-Canada, KoFlux, LBA, NECC, OzFlux, TCOS-Siberia, and USCCC networks provided data. Tristan Quaife provided the MATLAB code to download and organize MODIS data from the DAAC server. PCS acknowledges funding from the Marie Curie European Incoming International Fellowship (project number 237348, TSURF).

Table 1: Ecosystem type and geographic information for the 180 FLUXNET sites investigated here. GRA= grass, SAV = savanna (including woody savannas), CRO = crop, EBF = evergreen broadleaf forest, MF = mixed forest, ENF = evergreen needleleaf forest, DBF = deciduous broadleaf forest, WET = wetlands, SHRUB = shrublands. NA means that ecosystem type information was not available.

Site	**Vegetation**	**Latitude**	**Longitude**	**Site**	**Vegetation**	**Latitude**	**Longitude**
ATNeu	GRA	47.117	11.318	ITNon	DBF	44.69	11.089
AUFog	SAV	-12.542	131.31	ITPia	DBF	45.201	9.061
AUHow	SAV	-12.494	131.15	ITRen	ENF	46.588	11.435
AUTum	EBF	-35.656	148.15	ITRo1	DBF	42.408	11.93
AUWac	EBF	-37.429	145.19	ITRo2	DBF	42.39	11.921
BEBra	MF	51.309	4.5206	ITSRo	ENF	43.728	10.284
BEJal	MF	50.564	6.0733	JPMas	CRO	36.054	140.03
BELon	CRO	50.552	4.7449	JPTom	MF	42.739	141.51
BEVie	MF	50.306	5.9968	KRHnm	NA	34.55	126.57
BRBan	EBF	-9.8244	-50.159	KRKw1	MF	37.749	127.16
BRMa2	EBF	-2.6091	-60.209	NLCa1	GRA	51.971	4.927
BRSa3	EBF	-3.018	-54.971	NLLan	CRO	51.954	4.9029
BRSp1	SAV	-21.619	-47.65	NLLoo	ENF	52.168	5.744
BWGhg	SAV	-21.51	21.74	NLLut	CRO	53.399	6.356
BWGhm	SAV	-21.2	21.75	NLMol	CRO	51.65	4.639
BWMa1	SAV	-19.916	23.56	PLwet	WET	52.762	16.309
CACa1	ENF	49.867	-125.33	PTMi2	GRA	38.477	-8.0246
CACa2	ENF	49.87	-125.29	RUChe	MF	68.615	161.34
CACa3	ENF	49.535	-124.9	RUFyo	ENF	56.462	32.924
CAGro	MF	48.217	-82.156	RUZot	ENF	60.801	89.351
CAMer	SHRUB	45.409	-75.519	SEFaj	WET	56.265	13.554
CAOas	DBF	53.629	-106.2	SEFla	ENF	64.113	19.457
CAObs	ENF	53.987	-105.12	SENor	ENF	60.086	17.48
CAOjp	ENF	53.916	-104.69	SESk1	ENF	60.125	17.918
CAQcu	ENF	49.267	-74.036	SKTat	ENF	49.121	20.163
CAQfo	ENF	49.693	-74.342	TWTar	NA	24.031	120.69
CATP1	ENF	42.661	-80.56	UKAMo	WET	55.792	-3.2389
CATP2	ENF	42.774	-80.459	UKEBu	GRA	55.866	-3.2058
CATP3	ENF	42.707	-80.348	UKESa	CRO	55.907	-2.8586
CATP4	ENF	42.71	-80.357	UKGri	ENF	56.607	-3.7981
CHOe1	GRA	47.286	7.7321	UKHam	DBF	51.121	-0.86083
CHOe2	CRO	47.286	7.7343	UKHer	CRO	51.784	-0.47608
CNBed	EBF	39.531	116.25	USARb	GRA	35.546	-98.04
CNCha	MF	42.403	128.1	USARc	CRO	36.605	-97.488
CNDo1	GRA	31.517	121.96	USARM	GRA	35.55	-98.04
CNDo2	GRA	31.585	121.9	USAtq	WET	70.47	-157.41
CNDo3	GRA	31.517	121.97	USAud	GRA	31.591	-110.51
CNDu1	CRO	42.046	116.67	USBkg	GRA	44.345	-96.836
CNDu2	GRA	42.047	116.28	USBlo	ENF	38.895	-120.63
CNHaM	GRA	37.37	101.18	USBn1	ENF	63.92	-145.38
CNKu1	EBF	40.538	108.69	USBn2	DBF	63.92	-145.38
CNKu2	SHRUB	40.381	108.55	USBn3	SHRUB	63.923	-145.74
CNXfs	NA	44.134	116.33	USBo1	CRO	40.006	-88.292

CNXi1	GRA	43.546	116.68	USBo2	CRO	40.006	-88.292
CNXi2	GRA	43.554	116.67	USBrw	WET	71.323	-156.63
DEBay	ENF	50.142	11.867	USCaV	GRA	39.063	-79.421
DEGeb	CRO	51.1	10.914	USFmf	SAV	29.949	-97.996
DEGri	GRA	50.95	13.512	USFPe	ENF	35.133	-111.73
DEHai	DBF	51.079	10.452	USFR2	GRA	48.308	-105.1
DEHar	ENF	47.934	7.601	USFuf	ENF	35.09	-111.76
DEKli	CRO	50.893	13.523	USFwf	GRA	35.446	-111.77
DEMeh	MF	51.275	10.656	USGoo	GRA	34.25	-89.97
DETha	ENF	50.964	13.567	USHo1	ENF	45.204	-68.74
DEWet	ENF	50.453	11.458	USIB1	CRO	41.859	-88.223
DKFou	CRO	56.484	9.5872	USIB2	GRA	41.841	-88.241
DKLva	GRA	55.683	12.083	USIvo	WET	68.487	-155.75
DKSor	DBF	55.487	11.646	USKS1	ENF	28.458	-80.671
ESES1	ENF	39.346	-0.31881	USKS2	SHRUB	28.609	-80.672
ESES2	CRO	39.276	-0.31522	USLPH	SHRUB	46.083	-89.979
ESLJu	SHRUB	36.928	-2.7505	USMe1	ENF	44.316	-121.61
ESLMa	SAV	39.942	-5.7734	USMe2	ENF	44.499	-121.62
ESVDA	GRA	42.152	1.4485	USMe3	DBF	39.323	-86.413
FIHyy	ENF	61.847	24.295	USMe4	DBF	38.744	-92.2
FIKaa	WET	69.141	27.295	USMMS	ENF	44.579	-121.5
FISod	ENF	67.362	26.638	USMOz	ENF	44.452	-121.56
FRAur	CRO	43.549	1.1078	USNC1	SHRUB	35.812	-76.712
FRGri	CRO	48.844	1.9524	USNC2	ENF	35.803	-76.668
FRHes	DBF	48.674	7.0646	USNe1	CRO	41.165	-96.47
FRLam	ENF	44.717	-0.7693	USNe2	CRO	41.18	-96.44
FRLBr	CRO	43.493	1.2372	USNe3	ENF	40.033	-105.55
FRLq1	GRA	45.644	2.737	USNR1	CRO	41.165	-96.477
FRLq2	GRA	45.639	2.737	USOho	DBF	41.555	-83.844
FRPue	EBF	43.741	3.5958	USSO2	SAV	33.374	-116.62
HUBug	GRA	46.691	19.601	USSO3	SAV	33.377	-116.62
HUMat	GRA	47.847	19.726	USSO4	SHRUB	33.384	-116.64
IECa1	CRO	52.859	-6.9181	USSP1	ENF	29.738	-82.219
IEDri	GRA	51.987	-8.7518	USSP2	ENF	29.765	-82.245
ILYat	ENF	31.345	35.051	USSP3	ENF	29.755	-82.163
ISGun	DBF	63.833	-20.217	USSP4	ENF	29.803	-82.203
ITAmp	GRA	41.904	13.605	USSRM	SAV	31.821	-110.87
ITBCi	CRO	40.524	14.957	USSyv	MF	46.242	-89.348
ITCas	CRO	45.063	8.6685	USTon	SAV	38.432	-120.97
ITCol	DBF	41.849	13.588	USVar	GRA	38.413	-120.95
ITCpz	EBF	41.705	12.376	USWBW	DBF	35.959	-84.287
ITLav	EBF	43.305	11.271	USWCr	DBF	45.806	-90.08
ITLec	DBF	45.581	7.1546	USWi1	DBF	46.73	-91.233
ITLMa	ENF	45.955	11.281	USWi2	ENF	46.687	-91.153
ITMal	GRA	46.016	11.047	USWi8	DBF	46.722	-91.252
ITMBo	GRA	46.117	11.703	USWkg	GRA	31.736	-109.94
ITNoe	SHRUB	40.606	8.151	USWrc	ENF	45.82	-121.95

Table 2: The mean and standard deviation of radiation balance closure (C_{EB}) across different ecosystem types for the 180 sites in the FLUXNET database with measurements of available energy ($\sum(R_n - G)$) that sum to greater than zero. Numbers in parentheses are results after filtering for sites with questionable data products defined as $C_{EB} > 1.2$ or $C_{EB} < 0.5$. Three sites had no available ecosystem type information and are excluded here.

Vegetation type	n	C_{EB}
Crops	26 (22)	0.75 ± 0.19 (0.81 ± 0.12)
Shrubs*	9 (9)	0.88 ± 0.15 (0.88 ± 0.15)
Deciduous Broadleaf Forest	20 (18)	0.68 ± 0. 19 (0.73 ± 0.14)
Evergreen Broadleaf Forest	10 (10)	0.94 ± 0.16 (0.94 ± 0.16)
Evergreen Needleleaf Forest	49 (44)	0.83 ± 0.20 (0.82 ± 0.13)
Grasslands	34 (27)	0.94 ± 0.39 (0.87 ± 0.12)
Mixed Forest	10 (10)	0.75 ± 0.17 (0.75 ± 0.17)
Savanna+	12 (11)	0.95 ± 0.16 (0.92 ± 0.13)
Wetlands	7 (7)	0.73 ± 0.10 (0.73 ± 0.10)

WE_closure1_hh.m

Figures

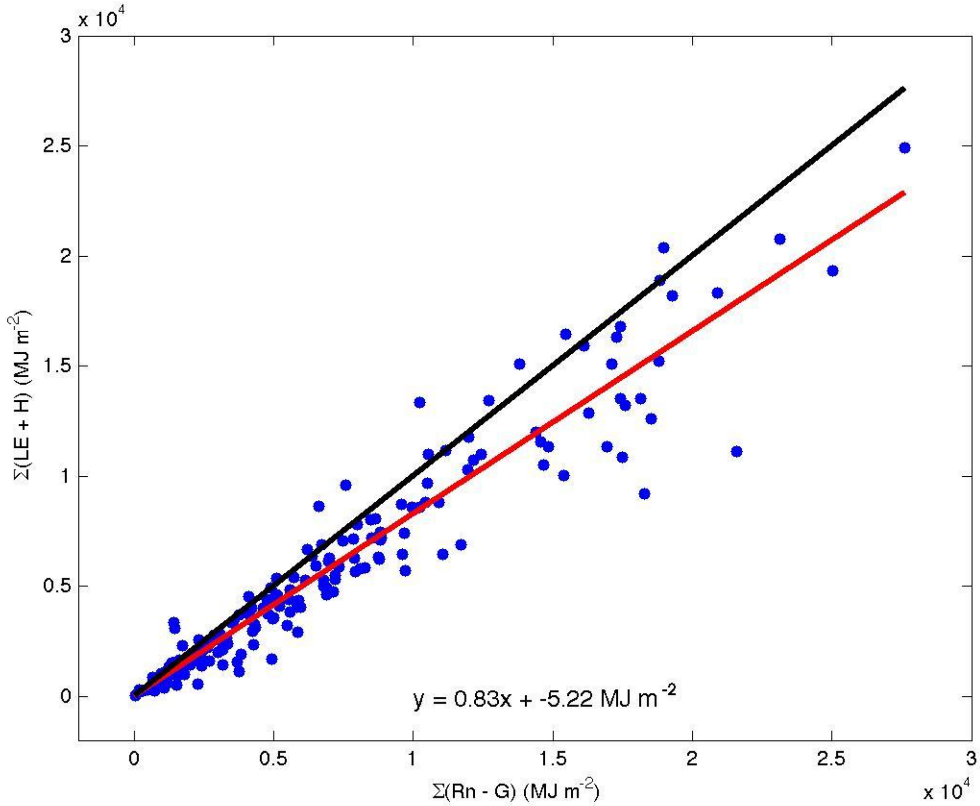

Figure 1: The relationship between the sum of available energy (net radiation, R_n minus soil heat flux, G) and the sum of surface fluxes of latent heat (λE) and sensible heat (H) for the 180 research sites in the FLUXNET database for which all four variables are measured and sum to a positive value.

WE_closure1_hh.m

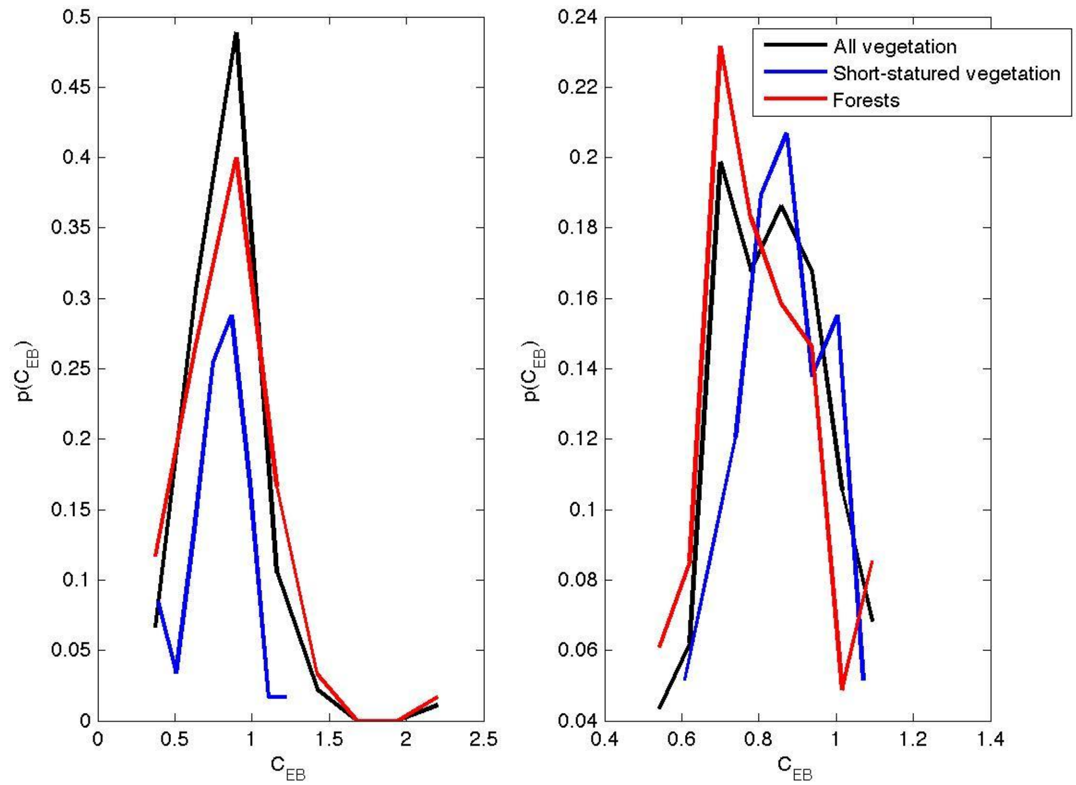

Figure 2: (a) The probability density function of the radiation imbalance (C_{EB}) for the 180 FLUXNET sites listed in Table 1, separated into non-forest and forest vegetation classes. Outliers (C_{EB}>1.2 and C_{EB}<0.5) are removed for the subsequent analyses to avoid sites with questionable data products, and the corresponding pdfs are plotted in (b).

WE_closure1_hh.m

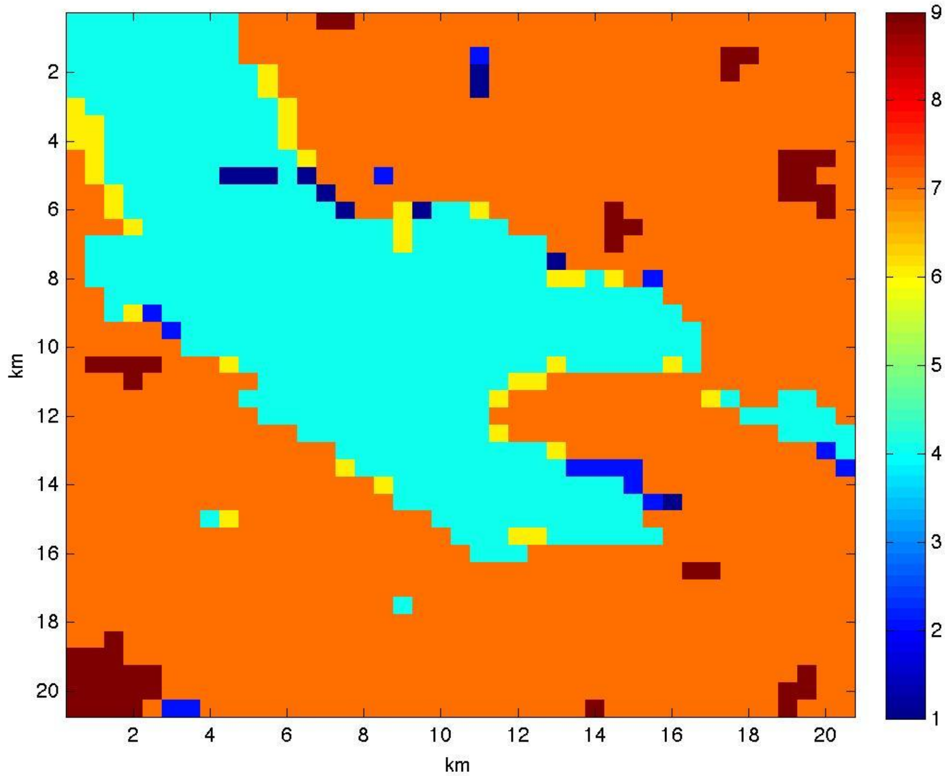

Figure 3: MODIS MCD12Q1 plant functional type for the 20 × 20 km area surrounding the Hainich deciduous broadleaf forest, Germany for 2006. The entropy of plant functional type, H(PFT), for this image is 0.90.

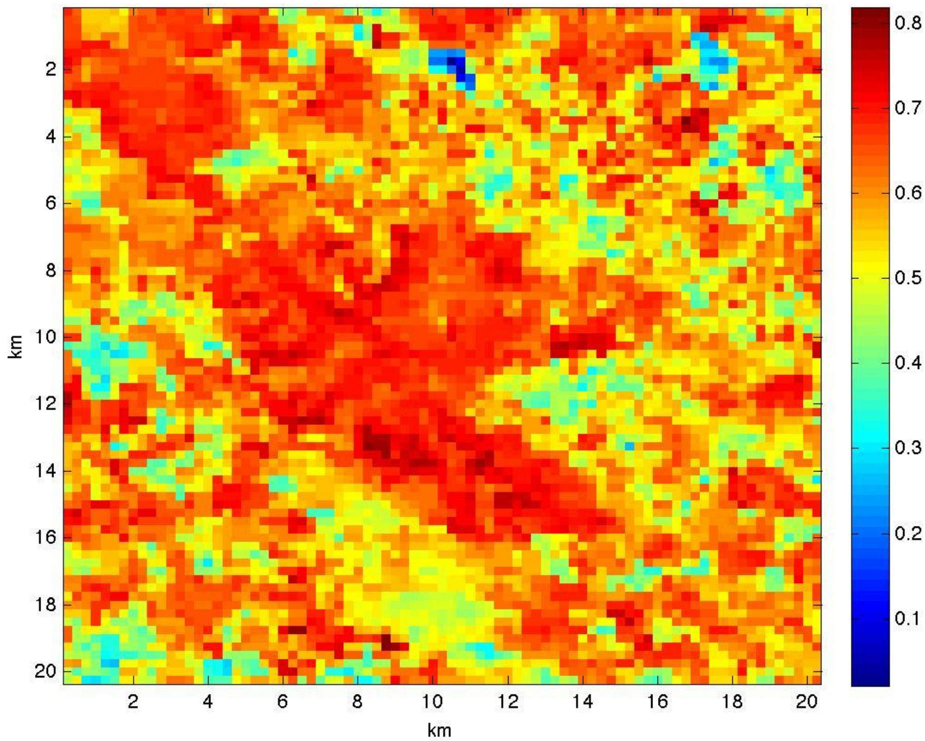

Figure 4: The MODIS MOD13Q1 enhanced vegetation index (EVI) for a 20 $\times$ 20 km area surrounding the Hainich deciduous broadleaf forest, Germany, measured on DOY 177, 2005. For reference, the variance of EVI, $\sigma^2(EVI)$, of this image is 8.6×10^{-3}.

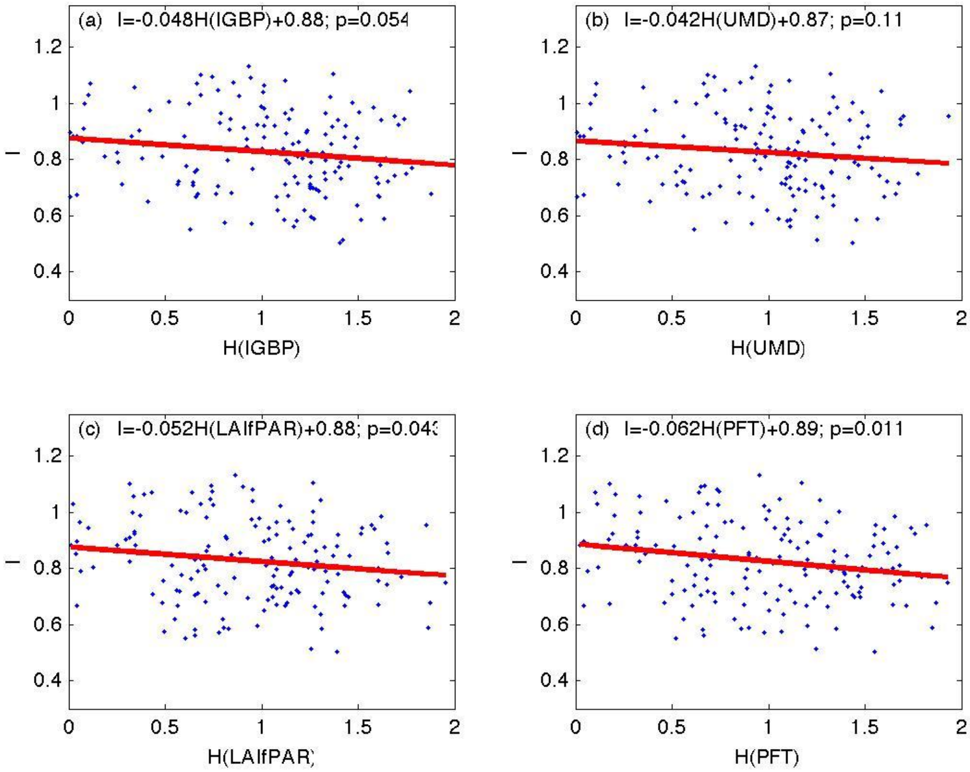

Figure 5: The imbalance (C_{EB}) of the radiation balance closure for 180 FLUXNET eddy covariance research sites plotted as a function of the Shannon entropy [$H(X)$] of MODIS-observed land cover classifications after the International Biosphere-Geosphere Program (IGBP, a), the University of Maryland product (UMD, b), leaf area index/fraction of absorbed photosynthetically active radiation (LAIfPAR,c) and plant functional type (PFT, d).

References

Aubinet M, et al. Direct advection measurements do not help to solve the night-time CO2 closure problem: Evidence from three different forests. Agric. For. Meteorol. (2010).

Aubinet M, et al. Estimates of the annual net carbon and water exchange of forests: The EUROFLUX methodology. Advances in Ecological Research (2000) 30:113-175.

Baldocchi D, et al. FLUXNET: A new tool to study the temporal and spatial variability of ecosystem-scale carbon dioxide, water vapor, and energy flux densities. Bull. Amer. Meteorol. Soc. (2001) 82:2415-2434.

Baldocchi DD. 'Breathing' of the terrestrial biosphere: lessons learned from a global network of carbon dioxide flux measurements systems, Turner Review. Australian Journal of Botany (2008) 56:1-26.

Barr AG, Morgenstern K, Black TA, McCaughey JH, Nesic Z. Surface energy balance closure by the eddy covariance method above three boreal forest stands and implications for the measurement of CO2 flux. Agric. For. Meteorol. (2006) 140:322-337.

Cava D, Contini D, Donateo A, Martano P. Analysis of short-term closure of the surface energy balance above short vegetation. Agric. For. Meteorol. (2008) 148:82-93.

Falge E, et al. Gap filling strategies for long term energy flux data sets. Agric. For. Meteorol. (2001) 107:71-77.

Foken T. The energy balance closure problem: an overview. Ecol. Appl. (2008) 18:1351-1367.

Foken T, Wimmer F, Mauder M, Thomas C, Liebethal C. Some aspects of the energy balance closure problem. Atmospheric Chemistry and Physics (2006) 6:4395-4402.

Gu L, et al. Influences of biomass heat and biochemical energy storages on the land surface fluxes and radiative temperature. Journal of Geophysical Research (2007) 112:D02107.

Heusinkveld BG, Jacobs AFG, Hostslag AAM, Berkowicz SM. Surface energy balance closure in an arid region: role of soil heat flux. Agric. For. Meteorol. (2004) 122:21-37.

Hollinger DY, et al. Albedo estimates for land surface models and support for a new paradigm based on foliage nitrogen concentration. Glob. Change Biol. (2009):doi: 10.1111/j.1365-2486.2009.02028.x.

Kanda M, Inagaki A, Letzel MO, Raasch S, Watanabe T. LES study of the energy imbalance problem with eddy covariance fluxes. Boundary-Layer Meteorology (2004) 110:381-404.

Law BE, et al. Environmental controls over carbon dioxide and water vapor exchange of terrestrial vegetation. Agric. For. Meteorol. (2002) 113:97-120.

Lee X. On micrometeorological observations of surface-air exchange over tall vegetation. Agric. For. Meteorol. (1998) 91:39-49.

Li ZQ, Yu GR, Wen XF, Zhang LM, Ren CY, Fu YL. Energy balance closure at ChinaFLUX sites. Science in China Series D - Earth Sciences (2005) 48:51-62.

Lindroth A, Molder M, Lagergren F. Heat storage in foret biomass improves energy balance closure. Biogeosciences (2009) 7:301-313.

Malhi Y, et al. Carbon dioxide transfer over a central Amazonian rain forest. Journal of Geophysical Research (1998) 103:31593-31612.
Mauder M, Jegede OO, Okogbue EC, Wimmer F, Foken T. Surface energy flux measurements at a tropical site in West-Africa during the transition from dry to wet season. Theoretical and Applied Climatology (2007) 89:171-183.
Meyers TP, Hollinger SE. An assessment of storage terms in the surface energy balance of maize and soybean. Agric. For. Meteorol. (2004) 125:105-115.
Oishi AC, Oren R, Stoy PC. Estimating components of forest evapotranspiration: a footprint approach for scaling sap flux measurements. Agric. For. Meteorol. (2008):1719-1732
Papale D, et al. Towards a standardized processing of Net Ecosystem Exchange measured with eddy covariance technique: algorithms and uncertainty estimation. Biogeosciences (2006) 3:571-583.
Reichstein M, et al. On the separation of net ecosystem exchange into assimilation and ecosystem respiration: review and improved algorithm. Glob. Change Biol. (2005) 11:1424-1439.
Ruppert J, Thomas C, Foken T. Scalar similarity for relaxed eddy accumulation. Boundary-Layer Meteorology (2006) 120:39-63.
Schäfer KVR, Oren R, Lai CT, Katul GG. Hydrologic balance in an intact temperate forest ecosystem under ambient and elevated atmospheric CO_2 concentration. Glob. Change Biol. (2002) 8:895-911.
Shannon CE. A mathematical theory of communication. Bell System Technical Journal (1948) 27:379-423 and 623-656.
Steinfeld G, Letzel MO, Raasch S, Kanda M, Inagaki A. Spatial representativeness of single tower measurements and the imbalance problem with eddy-covariance fluxes: results of a large-eddy simulation study. Boundary-Layer Meteorology (2006) 123:77-98.
Stoy PC, et al. Separating the effects of climate and vegetation on evapotranspiration along a successional chronosequence in the southeastern U.S. Glob. Change Biol. (2006) 12:2115-2135.
Twine TE, et al. Correcting eddy-covariance flux underestimates over a grassland. Agric. For. Meteorol. (2000) 103:279-300.
Vourlitis GL, Oechel WC. Eddy covariance measurements of CO_2 and energy fluxes of an Alaskan tussock tundra ecosystem. Ecology (1999) 80:686-701.
Wilson K, et al. Energy balance closure at FLUXNET sites. Agric. For. Meteorol. (2002) 113:223-243.
Yu G-R, Wen X-F, Sun X-M, Tanner BD, Lee X, Chen J-Y. Overview of ChinaFLUX and evaluation of its eddy covariance measurement. Agric. For. Meteorol. (2006) 137:125-137.